Separation Science and Technology
Publication details, including instructions for authors and subscription information:
http://www.informaworld.com/smpp/title~content=t713708471

H_2 Separation From H_2/N_2 and H_2/CO Mixtures with Co-Polyimide Hollow Fiber Module

Seung-Hak Choi[a]; Adele Brunetti[a]; Enrico Drioli[ab]; Giuseppe Barbieri[a]
[a] Institute on Membrane Technology (ITM-CNR), National Research Council, c/o The University of Calabria, Rende, CS, Italy [b] The University of Calabria - Department of Chemical Engineering and Materials, Rende, CS, Italy

Online publication date: 20 December 2010

To cite this Article Choi, Seung-Hak , Brunetti, Adele , Drioli, Enrico and Barbieri, Giuseppe(2011) 'H_2 Separation From H_2/N_2 and H_2/CO Mixtures with Co-Polyimide Hollow Fiber Module', Separation Science and Technology, 46: 1, 1 — 13
To link to this Article: DOI: 10.1080/01496395.2010.487847
URL: http://dx.doi.org/10.1080/01496395.2010.487847

Separation Science and Technology, 46: 1–13, 2011

ISSN: 0149-6395 print/1520-5754 online
DOI: 10.1080/01496395.2010.487847

Taylor & Francis
Taylor & Francis Group

H_2 Separation From H_2/N_2 and H_2/CO Mixtures with Co-Polyimide Hollow Fiber Module

Seung-Hak Choi,[1] Adele Brunetti,[1] Enrico Drioli,[1,2] and Giuseppe Barbieri[1]

[1]*Institute on Membrane Technology (ITM–CNR), National Research Council, c/o The University of Calabria, Rende, CS, Italy*

[2]*The University of Calabria - Department of Chemical Engineering and Materials, Rende, CS, Italy*

A lab-scale membrane module, packed with more than 150 hollow fibers of P84® co-polyimide, was used for the separation of hydrogen mixtures. The ideal membrane performance was analysed with pure gases (H_2, N_2, CO, CO_2, CH_4) and H_2/N_2 and H_2/CO mixtures at 50°C and up to 6 bar. Significant differences were observed between ideal selectivities and separation factors of mixtures. In gas mixture experiments, no variation of hydrogen flux was observed among the different feeds, whereas the permeance of the less permeating species, i.e., N_2 and CO, was significantly higher than that measured with pure gases. A linear dependence of H_2 recovery on the stage cut was observed in the whole feed pressure range investigated. No differences in the behavior of the membrane versus the two different mixtures were observed. A higher separation factor was obtained when H_2 was mixed with N_2 rather than CO, in agreement with the trend followed by ideal selectivity values, since the one of H_2/N_2 was 78, a bit higher than that of H_2/CO (60). However, the hydrogen concentration in the permeate also reached 90% molar. The performances of a membrane system were compared with PSA and cryogenic, considering two metrics of process intensification.

Keywords (P84) co-polyimide membrane; H_2 mixtures; H_2 separation; hollow fiber module

INTRODUCTION

In the last few years the potentialities of membrane operations have been widely recognized. The attention to the Process Intensification strategy, as the best available approach for an appropriate sustainable industrial growth (1), has contributed to confirming membrane engineering as a powerful tool to realize this strategy in the best way. Today membrane technology for gas separation is a well-consolidated technique, in various cases competitive with traditional operations. Separation of air components, H_2 recovery from refinery industrial gases, natural gas dehumidification, and the separation and recovery of CO_2 from biogas and natural gas are some examples in which membrane technology is already applied at pilot or industrial level (2). The hydrogen upgrading in refineries is currently carried out by means of pressure swing adsorption (PSA) and cryogenic separation processes. However, the application of membrane systems for this type of separation is rapidly evolving on a commercial level, owing to the advantages related to the low capital costs, low energy requirements, and modularity (3). In the literature various polymers and polymeric membranes (4,5,6,7) are indicated, exhibiting interesting properties in terms of permeance and ideal selectivity. However, the majority of them are only available at lab scale and membranes with good permselectivities and high mechanical resistances are necessary.

Polyimides (PI) are a successful example of an industrially applied membrane material. Generally, polyimides are synthesized by polycondensation reactions of dianhydrides with diamines and thermally stable polymer with good correlation between permeability and permselectivity (8). P84® co-polyimide (BTDA-TDI/MDI, 3,3′4,4′-benzophenone tetracarboxylic dianhydride, and 80% methylphenylene diamine +20% methylene diamine) is one of the most selective glassy polymers with high heat resistance and excellent mechanical and chemical properties.

Barsema et al. (9) reported the permeation properties and the plasticization behavior of both pure gases and gaseous mixtures (CO_2/N_2) for dense flat sheet and asymmetric hollow fiber BTDA-TDI/MDI membranes. According to their experimental results, no plasticization was observed when a CO_2/N_2 (80/20 vol.%) mixture was fed to the P84 co-polyimide hollow fiber membranes for pressures up to 30 bar. Ren et al. (10,11) investigated the effects of the thermodynamic characteristics and rheological properties of the dope solution within the spinneret and other spinning conditions such as the air gap, the volume ratio of the dope solution to the bore fluid, and the casting temperature on the performance and morphology. They

Received 18 January 2010; accepted 20 April 2010.

Address correspondence to Giuseppe Barbieri, c/o The University of Calabria – Cubo 17C, via Pietro BICCI, Rende 87036, Italy. Fax: +39 0984 402103. E-mail: g.barbieri@itm.cnr.it

introduced a concept of "approaching ratio" to explain thermodynamic characteristic of the polymer solution.

In this work, the choice of the PI and, in particular of the P84 type, as polymer for producing membrane hollow fiber for H_2 separation was made taking into account not only the high selectivity (9) and high thermal and mechanical stability, but also considering that the separation of H_2 from its mixtures with this polymer has not yet been particularly investigated. Only Peer and co-workers (12) studied the separation of H_2 from syngas at different feed conditions such as feed pressure, feed flow rate, and operating temperature, using a small membrane made with commercial polyimide (supplied from UBE Industries Ltd., Japan).

The P84 membrane properties were measured, first on a single fiber, for evaluating the suitability of this material for H_2 separation; then, the 165 hollow fiber were packed into the module and the ideal transport properties (permeance and ideal selectivity) were measured with pure gases (H_2, CH_4, CO_2, CO and N_2).

The key issue for the application of polymeric membranes in the gas separation is to study the performance of the module considering gas mixtures of industrial interest (13). Generally, the majority of the papers present in the literature refers to the transport properties measured in ideal conditions, such as pure gases at low stage cut. However, in many cases these values differ, sometimes significantly, from that obtained feeding gas mixtures (14).

In this work, the transport properties of the prepared P84 hollow fibers module were measured feeding binary gas mixtures (H_2/N_2 and H_2/CO). The separation factor, the hydrogen recovery and final H_2 concentration in the permeate were measured at 50°C, up to 6 bar of feed pressure and keeping to 1 atm the permeate pressure, for evaluating the capability of the membrane to separate mixtures of industrial interest.

MATERIALS AND METHODS

Materials

The selected membrane material, BTDA-TDI/MDI co-polyimide (trade name: P84), was purchased from HP polymer GmbH, Austria. The chemical structure of P84 is shown in Fig. 1. N-Methyl-2-pyrrolidone (NMP, Carlo Erba, Italy, >99.5%) was used as solvent. Tap water was used as external coagulant, while ultrapure water or its mixtures with NMP were used as the bore fluid. Poly (dimethylsiloxane) (PDMS, RTV 615, GE Bayer Silicones) and n-hexane (Carlo Erba, Italy, >99%) were used to seal the defects on hollow fibers. Two-component epoxy resin (Stycast 1266, Emerson & Cuming, Belgium) was used for potting in the membrane module preparation.

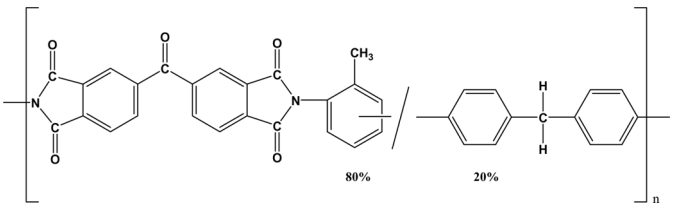

FIG. 1. Chemical structure of P84 (BTDA-TDI/MDI) co-polyimide.

Membrane and Module Preparation

P84 co-polyimide was dissolved in the solvent (NMP) and then stirred for 1 day at room temperature. The homogeneously prepared polymer solution was then transferred into the dope tank, kept at a constant temperature of 30°C, and finally degassed under vacuum.

Hollow fibers were spun by the well-known dry/wet phase inversion process with the spinning apparatus which is illustrated in Fig. 2. The dope solution was fed to the spinneret by a gear pump and the bore fluid by a peristaltic pump. The extruded fibers passed through a certain length of air-gap and then coagulated in a water bath with continuous circulation to control the temperature and to avoid local build-up of the solvent concentration. The nascent fiber was pulled out of the coagulation bath by take-up rolls rotating at adjustable speed. Finally, the continuous bundle of fibers was cut in pieces of about 40 cm and transferred in a circulating hot water bath kept at 50°C for at least 24 hours. The washed fibers were dried in air for over 24 hours and dip-coated with a 2 wt.% poly(dimethylsiloxane) solution in n-hexane to seal the defects on the fibers.

A lab-scale P84 hollow fiber module 20 cm long containing 165 fibers was fabricated. The effective fiber length and membrane area were 16 cm and ca. 388 cm^2, respectively. Pure or mixed feed gas was introduced to the shell side of fibers and permeate was collected in the bore side.

Membrane Characterization and Gas Separation Experiments

The morphology of the prepared P84 hollow fiber membranes was determined by scanning electron microscope (SEM, FEI QUANTA 200 F). The pure gas permeation properties of the hollow fiber membrane were analyzed using 6 different pure gases (He, H_2, N_2, O_2, CH_4, and CO_2) at 35°C. On the other hand, pure gases (H_2, N_2, CO_2, CO, and CH_4) and binary gas mixtures (H_2/N_2 and H_2/CO) were used to characterize the separation performance of prepared membrane module. Furthermore, the effects of operating the trans-membrane pressure difference, the feed flow rate, and feed composition on the permeating flux, H_2 recovery and purity, and the separation factor were analyzed with membrane module.

The transport properties of the membranes and module were investigated by feeding pure gases (H_2, N_2, CO_2, CO, and CH_4) and binary mixtures (H_2/N_2 and H_2/CO), respectively at different operating trans-membrane pressure differences in order to measure the permeating flux

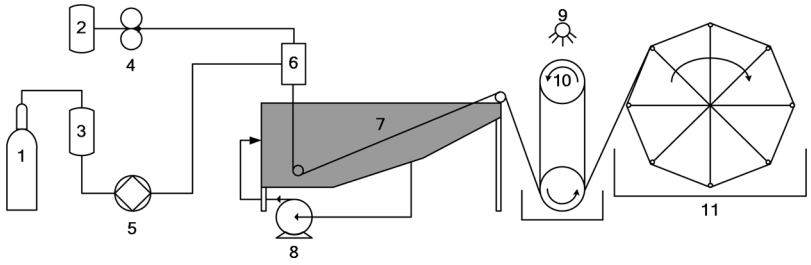

FIG. 2. Schematic drawing of the spinning setup. 1: N_2 gas cylinder, 2: bore fluid tank, 3: dope tank, 4: bore fluid pump, 5: gear pump, 6: spinneret, 7: external coagulation bath, 8: circulation pump, 9: water spray, 10: take-up rollers, 11: spool.

TABLE 1
Operating parameters

Temperature	50°C
Pressure	Feed/Retentate: up to 6 bar Permeate: 1 bar
Feed flow rate	0.6–3.9 dm^3(STP) h^{-1}
Feed composition	Pure gases. H_2, N_2, CO_2, CO, CH_4 Mixtures [%molar] H_2:CO = 30:70 H_2:N_2 = 30:70

and evaluate the membrane properties such as permeance, ideal selectivity and separation factor. Table 1 reports the operating conditions adopted during the experiments. All the experiments were carried out at 50°C, varying the feed pressure up to 6 bar and maintaining atmospheric the permeate pressure. Both the mixtures considered in the experiments contain 30% of H_2 and this choice was made on the basis of the typical composition of the methane partial oxidation outlet stream for which these membranes could represent a potential application(15). The experimental apparatus is schematically shown in Fig. 3.

The core of the system is the hollow fiber membrane module placed in a furnace. The hollow fibers were sealed on a support by means of epoxy resin and, then, this system (picture reported in Fig. 3) was assembled in the module. The net membrane area available for permeation is ca. 388 cm^2. The stainless steel module is tubular with feed and permeate sides. Both of them have two inlets/exits: the feed and retentate on one side and the permeate and sweep on the other side. During the experiments no sweep gas was used and the sweep and permeate exits were connected constituting only one exit. The two mixtures of set composition obtained by the pure gases from different cylinders (at least 99.99% purity) were fed to the hollow fiber by means of mass flow controllers. A back pressure regulator on the retentate line and a gauge on the feed line allowed the required trans-membrane pressure difference to be operated in the module. The presence of a gauge also on the feed line allowed the eventual presence of pressure drops to be estimated. The retentate and permeate flow rates were measured by means of two bubble soap flow meters. Permeation measurements with pure gases were carried out using the pressure drop method, consisting in measuring the gas permeating flow rate for an imposed feed pressure, keeping the retentate side closed. When the mixtures were fed into the module, the measurements were performed by means of the concentration gradient method, forcing a part of the feed stream to permeate the membrane and also measuring the retentate flow rate.

The experimental measurements taken at 50°C allowed the membrane permeance to be estimated. The permeance (Eq. (1)) is the ratio of the flux and driving force and was evaluated as the slope of the linear fitting through the axes

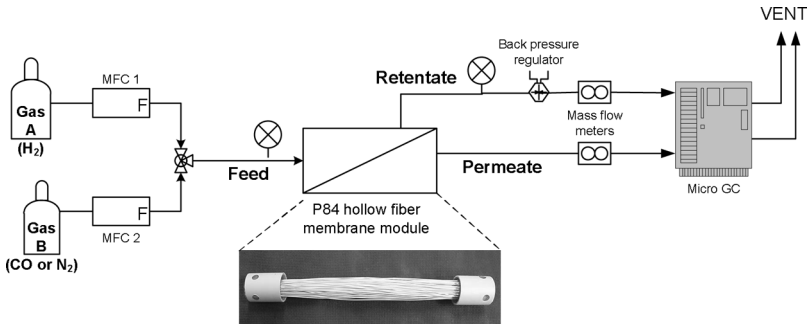

FIG. 3. Experimental setup for binary mixture gas permeation test.

origin of the permeating flux (Eq. (2)) as a function of the corresponding driving force (Eq. (3)).

$$\text{Permeance}_i = \frac{\text{Permeating flux}_i}{\Delta P_i^{TM}}, \text{dm}^3(\text{STP})\text{m}^{-2}\,\text{h}^{-1}\,\text{bar}^{-1} \quad (1)$$

$$\text{Permeating flux}_i = \frac{\text{Permeate flow rate}_i}{\text{membrane area}}\ \text{dm}^3(\text{STP})\text{m}^{-2}\,\text{h}^{-1} \quad (2)$$

$$\text{Driving force} = \Delta P_i = P_i^{\text{Retentate}} - P_i^{\text{Permeate}}, \text{bar} \quad (3)$$

The ratio between the membrane permeances of two gases is the ideal selectivity (Eq. 4). The separation factor (Eq. 5) expresses the relative enrichment in the permeate stream with respect to the feed composition when a gas mixture is fed to the membrane system. It is important to well distinguish between ideal selectivity and the separation factor. The first one is calculated from the pure gas permeances measured in ideal conditions and it represents a property of the material. The separation factor indicates the actual performance of the membrane module and it depends on several parameters not only related to the material properties but also to the whole module conditions. Therefore parameters such as the feed and permeate pressures, the stage cut, the module configuration, and the mixture composition, become crucial variables affecting the separation factor.

$$\text{Ideal selectivity}_{ij} = \frac{\text{Permeance}_i}{\text{Permeance}_j} \quad (4)$$

$$\text{Separation factor}_{ij} = \frac{\left(\frac{x_i^{\text{Permeate}}}{x_j^{\text{Permeate}}}\right)}{\left(\frac{x_i^{\text{Feed}}}{x_j^{\text{Feed}}}\right)} \quad (5)$$

The results obtained with the mixture experiments were described also in terms of H_2 recovery (Eq. (6)) and H_2 concentration in the permeate in the permeate side and analysed as a function of feed pressure and the stage cut, defined as in Eq. (7).

$$H_2\ \text{recovery} = \frac{H_2\ \text{flow rate in the permeate}}{H_2\ \text{feed flow rate}} \quad (6)$$

$$\text{Stage cut} = \frac{\text{Permeate flow rate}}{\text{Feed flow rate}} \quad (7)$$

Comparison of the Membrane Systems with the Traditional Separation Systems

In order to evaluate the suitability of this membrane type for the hydrogen separation, a comparison with two traditional separation operations, actually used in industries, such as PSA (pressure swing adsorption) and cryogenic was made. The three units were compared considering not only the hydrogen recovery and purity, but also introducing two interesting metrics, currently used for giving an immediate idea of the gain offered by an innovative operation with respect to the traditional one. The *mass intensity* (16,17) and the productivity to footprint ratio were calculated as reported below. The mass intensity (Eq. (8)), more generally defined, takes into account the yield, stoichiometry, and feedstocks and expresses this on a weight/weight basis rather than a percentage. In the ideal situation, mass intensity would\approach 1. This means a good material exploitation and, thus, an intensified process with a lower impact on the global ecosystem (18). The productivity to footprint ratio (Eq. (9)) calculated for the membrane technology is very interesting in the Process Intensification logic. It considers the impact of the innovative technology in terms of land occupied by the installation. Therefore, the higher the indicator the more intensified is the process.

Mass Intensity

$$\text{Mass Intensity} = \frac{\text{Total inlet mass}}{H_2\ \text{mass in permeate}} \quad (8)$$

Productivity Footprint

$$\frac{\text{Productivity}}{\text{Footprint}} = \frac{H_2\ \text{mass in permeate}}{\text{Footprint}} \quad (9)$$

In this work, four different case studies related to the membrane module have been considered in the calculations. The first two refer to experimental results effectively achieved in the experimental campaign carried out in this work. The last two contain some results such as H_2 recovery and stage cut extrapolated from the experimental data, but considering a higher feed pressure and vacuum on the permeate side. Table 2 lists the operating conditions and the membrane properties related to the chosen case studies.

Nonlinear behavior such as that due to the CO_2 plasticization at a higher CO_2 partial pressure needs to be measured and then introduced in the model for simulations at a higher pressure. Non-linear effect was not observed in the range of low pressure operated. The simulation of membrane gas separation with PSA or cryogenic was performed up to a pressure little bit higher the total operating pressure used in the experiments.

TABLE 2
Membrane properties (measured) and corresponding operating conditions (experimentally used: cases 1 and 2; simulated cases 3 and 4) of the case studies chosen for the calculations

	Case 1	Case 2	Case 3	Case 4
H_2 Permeance, dm^3 (STP) $m^{-2} h^{-1} bar^{-1}$	9.94	11.8	9.94	11.8
Separation factor, -	6	20	6	20
Stage cut, %	27	9	35	20
Feed pressure, bar	6		10	
Permeate pressure, bar	1		0.2	
Temperature,°C	50			
Feed composition, [%molar]	H_2: N_2 = 30:70			

RESULTS AND DISCUSSION

Morphological Characteristics and Pure Gas Permeation Properties

Figure 4 illustrates the typical SEM images of prepared P84 co-polyimide hollow fiber membrane. The membrane has a typical asymmetric morphology, with a finger-like structure near the inner and the outer surface and with a sponge-like structure in the middle of the wall. The thickness of a membrane can be measured using a SEM picture but this measurement is, however, along a specific radius in a specific cross section of the membrane. An average value on a whole membrane area for a symmetric membrane can be evaluated by the relationship:

$$\text{Permeance} = \frac{\text{Permeabiltiy}}{\text{thickness}} \tag{10}$$

In fact, a permeance measurement is enough since the permeability of the polymer is known. The same relationship can be used for asymmetric membranes using permeance measurement of a single gas of more than one gas. The slope of the linear regression between the permeance and the permeability for several gases gives the ''effective membrane thickness'' (19). This method is also valid for asymmetric membranes when the permeability and permeance are referred to single gas measurements. In this case, the porous structure just supports the skin dense layer and no concentration polarization occurs in the support. On the contrary, if the permeance is measured using a gas mixture the method suffers with the effect of the concentration polarization and, thus, cannot be applicable. Using the above method, the P84 co-polyimide hollow fiber membrane has an effective thickness of approximately 1.03 μm utilizing the experimental data of six different gases.

As initial indication of the suitability of the membrane material for an H_2 separation it is important to measure the membranes transport properties (permeance and ideal selectivity) of the co-polyimide hollow fibers. For this reason, different permeation measurements with different pure gases (H_2, N_2, CO_2, CO, and CH_4) were carried out at 50°C, in a pressure range of 2–6 bar.

The permeating flux of each gas increased linearly with the correspondent permeation driving force; therefore, a constant permeance value was assumed for each gas, since the difference among experimental results and linear regression through the axes origin (i.e., the permeance) was lower than 2%. These results are reported in Table 3 in terms of permeance of each gas and hydrogen selectivity versus the other gases. The H_2 permeance was significantly higher than those of the other gases and the membrane

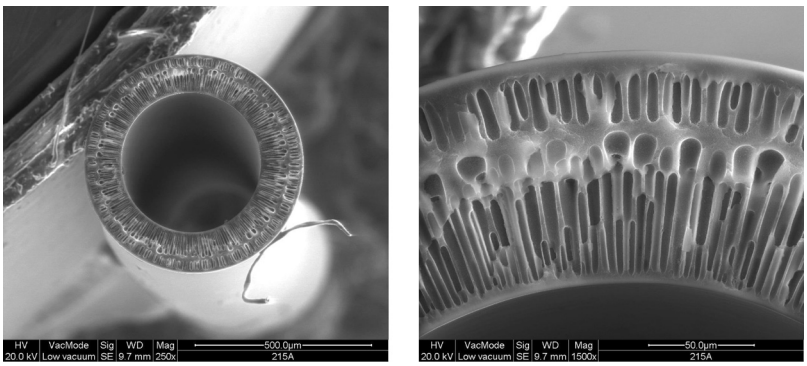

FIG. 4. Experimental setup for binary mixture gas permeation test.

TABLE 3
Pure gas permeance and their ideal selectivity of prepared P84 hollow fiber membrane module at 50°C

Gas species	Permeance, $dm^3(STP)\ m^{-2}\,h^{-1}\,bar^{-1}$	Permeance, pico–mol $m^{-2}\,s^{-1}\,Pa^{-1}$	H_2/i Ideal selectivity, -
H_2	12.0 ± 0.096	1480 ± 1.18	1
N_2	0.15 ± 0.0014	19.0 ± 0.17	78
CO	0.20 ± 0.001	24.9 ± 0.02	60
CH_4	0.16 ± 0.0003	20.2 ± 0.04	73
CO_2	$1.75. \pm 0.0014$	202 ± 0.17	7

showed good H_2/N_2, H_2/CO, and H_2/CH_4 ideal selectivities, whereas the H_2/CO_2 and CO_2/N_2 selectivities were not so consistent. On the basis of these results the investigation of the potential application of co-polyimide hollow fibers as a suitable alternative for interesting industrial gas separation processes considering only H_2/N_2 and H_2/CO mixtures was decided. The first was chosen due to the high selectivity obtained, the second since it has not been sufficiently investigated yet in the literature.

The polyimide membranes show acceptable permeance and superior selectivity, as many published papers already report. Table 4 summarizes the gas permeation properties of the P84 hollow fiber membranes and modules in comparison with literature data. In particular, the upper part of the table compares the permeability measured on a single fiber, whereas in the second part of the table a comparison in terms of module permeance is shown.

The permeability shown by the P84-fiber prepared in this work agrees well with that measured by Barsema et al. (9) on a similar membrane, whereas it is more or less lower than others(20,4). However, the H_2/N_2 ideal selectivity of the fiber is closer or higher than those of the other literature works, except for the carbon molecular sieve-P84 (21) which exhibits a significantly higher selectivity. Furthermore, it must be pointed out that there are significant differences between the transport properties measured on a single fiber and that measured with a hollow fiber module. The main difference in making the module is the capability of producing several meters of hollow fiber exhibiting all the same properties and, thus, the defects on the whole membrane surface are very few. The membrane module realized in this work contains more than 160 fibers equivalent to ca. 25 m of active length. Comparing the permeance and selectivity measured on our module with respect to that reported in another work present in the literature (22) the P84 co-polyimide module shows significantly higher permeance values and H_2/N_2 ideal selectivity. The latter, in fact, is 78 with respect to 20 of the other works. This value is not so different from that measured with the single fiber which means that the defects on the whole membrane surface are very few.

Mixtures Experiments

The mixtures experiments were performed feeding to the membrane module $H_2{:}N_2 = 30{:}70$ and $H_2{:}CO = 30{:}70$ mixtures. In particular, experimental investigations were carried out at 50°C up to 6 bar of feed pressure, analysing the effect of feed flow rate and stage cut on the performances of the hollow fibers membrane module.

The permeation tests showed a linear dependence of the flux on the corresponding driving force for all the species analyzed. No change in H_2 permeance was observed with respect to the pure gas tests (Fig. 5), feeding the different mixtures. On the contrary, N_2 and CO permeances measured in mixtures were higher than the correspondent ones measured with the pure gases (Fig. 6). These might be explained taking into account that the hydrogen flux is, at least, one order higher than the ones of the other gases. This implies that the incidence of the deviation from the straight line obtained with the pure H_2 test is lower with respect to the ones of the other gases. However, further investigations are needed to explain this phenomenon.

The experiments with the H_2/CO mixture were carried out at a feed flow rate of 2.8 $dm^3(STP)\ h^{-1}$, whereas the effect of the feed flow rate on the performance of the membrane module were studied with H_2/N_2 mixture, ranging the feed flow rate from 0.6 to 3.9 $dm^3(STP)\ h^{-1}$. In this case, no change in the permeance measured feeding the mixture was observed varying the feed flow rate (Fig. 6). As a consequence, whether the H_2 permeance measured feeding the mixtures was quite similar to that measured with pure gas, N_2 and CO permeance significantly increased.

In order to evaluate the co-polyimide hollow fibers performance in the H_2/N_2 mixture separation, the separation factor (Eq. (5)) was calculated as a function of the stage cut (Eq. (7)). This parameter, defined as the ratio between the permeate flow rate and the feed flow rate, can be directly related to the extractive performance of the module and, thus, to the connection between the membrane area and the flow rate. A low stage cut assures ideal permeation behavior for the absence of variation of the species composition along the membrane module in the feed/retentate side. On the contrary, a high stage cut causes a profile in the species concentration. The separation factor obtained, ranging 5 to 20, was in all the cases significantly lower than the ideal selectivity ($H_2/N_2 = 78$) measured with pure gases. In particular, a decreasing trend of the separation factor with the stage cut was observed (Fig. 7). On the inlet of the hollow fiber module, the permeation of H_2, in this case the more permeable species, is much favored having its correspondent maximum driving force. Along the module length the H_2 profile in the retentate side decreases due

TABLE 4
Comparison of the gas permeation properties of this study with those reported in the literature

Materials	Temperature (°C)	He	H_2	N_2	O_2	CH_4	CO_2	CO	H_2/N_2 ideal selectivity	Ref.
		Permeability[a], $mm^3(STP)\ m^{-2}\ h^{-1}\ bar^{-1}$; (Barrer)								
P84-fiber	25	17.4 (6.45)	14.3 (5.29)	0.13 (0.05)	0.58 (0.22)	0.32 (0.05)	2.8 (1.05)	–	106	This study
P84	25	19.3 (7.15)	–	0.06 (0.024)	0.57 (0.21)	–	3 (1.10)	–	–	(10)
Carbon molecular sieve-P84	40	27.4 (10.15)	43.5 (16.10)	0.06 (0.023)	0.75 (0.28)	0.07 (0.025)	2.6 (0.96)	–	712	(23)
Matrimid 5218	35	–	48 (17.75)	0.43 (0.16)	–	0.41 (0.15)	14.5 (5.39)	–	111	(21)
Polyimide-Ube	60	108 (40)	135 (50)	1.6 (0.6)	8.1 (3)	1.1 (0.40)	35 (13)		83	(5)
Kapton®	30	–	4.3 (1.6)	–	–	0.11 (0.04)	0.76 (0.28)	–	–	(22)
		Permeance, $dm^3(STP)\ m^{-2}\ h^{-1}\ bar^{-1}$; (GPU)							H_2/N_2 ideal selectivity	
P84-module	50	–	12 (4.44)	0.15 (0.056)		0.16 (0.059)	1.75 (0.65)	0.20 (0.074)	78	This study
P84	25	3.16 (1.17)	2.78 (1.03)	0.135 (0.05)	0.22 (0.08)	0.189 (0.07)	0.49 (0.18)	–	20	(24)

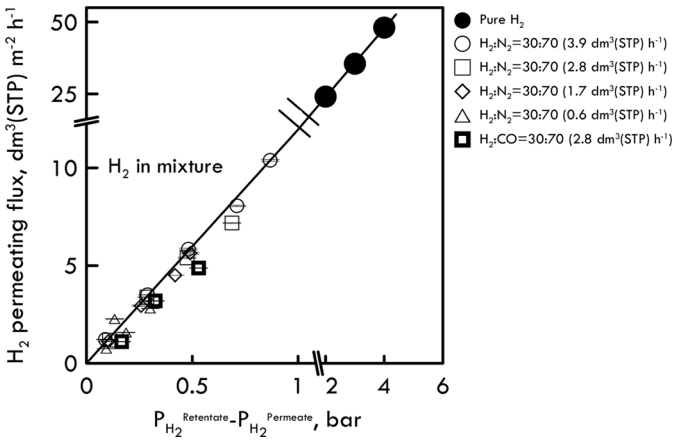

FIG. 5. H_2 permeating flux as a function of correspondent ΔP_{H2} at different feed flow rates. Measured data: open and full symbol for pure gas or gas mixture as feed streams, respectively. Line: linear regression through the axes origin.

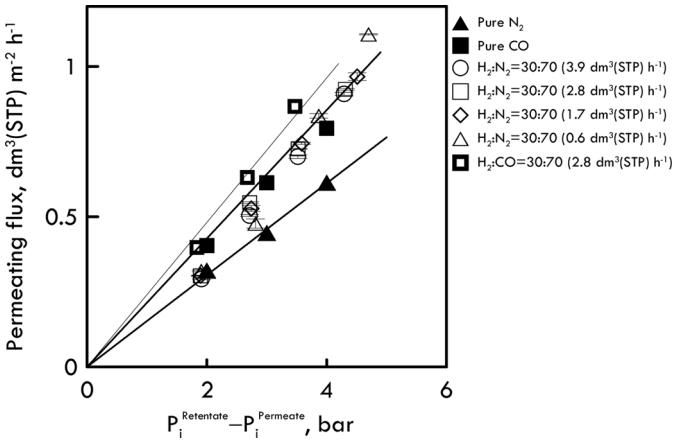

FIG. 6. Permeating flux of N_2 and CO as pure and in mixture as a function of correspondent ΔP_i for different values of feed flow rate. Symbols: measured data; lines: linear regression through the axes origin.

to its permeation as well as its correspondent driving force. On the contrary, the profile of the less permeable specie (N_2) increases as well as its driving force and, as a consequence, the N_2 permeates near the module end much more than at the entrance. These opposite effects produce a reduction of the separation factor with the stage cut, since it represents the extractive performance of the system. The higher separation factor was measured at the higher feed pressure, for the same value of stage cut (Fig. 7). The higher the feed pressure the higher the partial pressure and thus the driving force of both species in the retentate side. As a consequence, the H_2 is much more favored to permeate the membrane and the separation factor increases.

The concept related to the dependence of the separation factor on the stage cut can be better clarified considering Fig. 8, where the H_2 concentration in the permeate is shown as a function of the correspondent driving force, for different feed flow rates. Considering the curve at 0.6 dm^3(STP) min^{-1}, the H_2 concentration in the permeate increases with the driving force up to reach a maximum. An increase of the driving force favors the permeation through the membrane of the most permeable species; however, when the main part of hydrogen is permeated through the membrane, a further increase in the driving force, (produced increasing the feed pressure) causes the permeation also of the other species present in the retentate, with a consequent reduction of the H_2 molar fraction. This trend is much less evident than the feed flow rate increases. For a defined membrane area, an increase of the feed flow rate implies a lower residence time of the feed stream in the membrane module, therefore a lower fraction of the feed permeates. This means that the permeation of the more permeable specie is favored and, as a consequence the H_2 concentration in the permeate stream is higher, at the same driving force. For a low feed flow rate, the

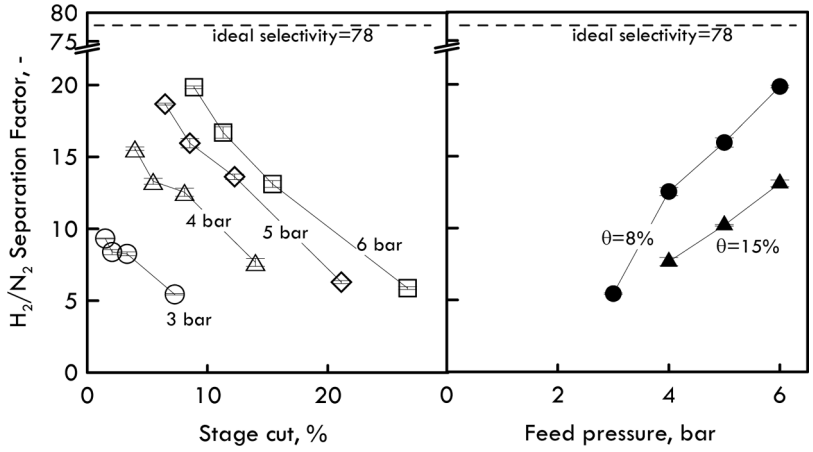

FIG. 7. H_2/N_2 separation factor as a function of stage cut and feed pressure, respectively. Mixture H_2:N_2 = 30:70.

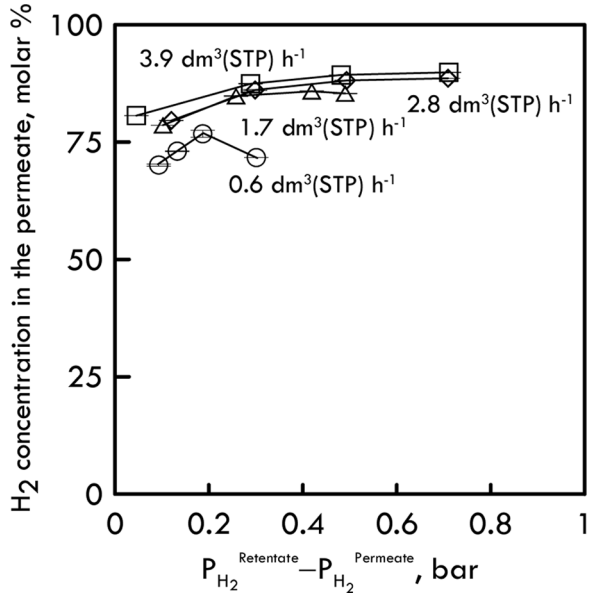

FIG. 8. H_2 concentration in the permeate as a function of ΔP_{H2} for different values of feed flow rate. Mixture H_2:N_2 = 30:70.

residence time is higher, therefore not only H_2 but also N_2 permeate with a consequent reduction of the H_2 concentration as well as of the hydrogen driving force (Fig. 8).

Figure 9 shows the H_2 recovery measured as a function of stage cut, at different feed pressures. A linear dependence of the H_2 recovery on the abscissa was observed for all the values of feed pressure considered. At a low stage cut, only a small part of the hydrogen fed is recovered in the permeate, since the feed flow rate is oversized with

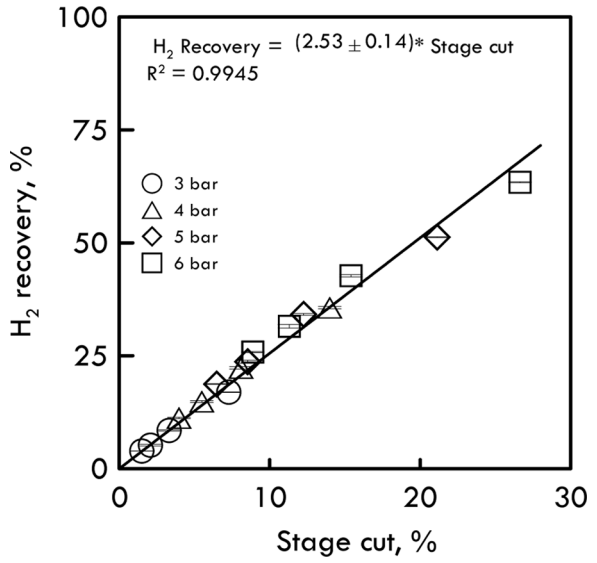

FIG. 9. Mixture H_2:N_2 = 30:70. H_2 recovery as a function of stage cut for different values of feed pressure.

respect to the membrane area available and, thus, to the extractive capacity of the membrane module; the higher the stage cut the higher the H_2 fraction recovered in the permeate.

The stage cut can be controlled by changing the feed flow rate at constant pressure and/or by changing feed pressure at constant feed flow rate. An increase in the feed pressure leads to a higher permeation and, in other words, to an increase in the stage cut. As a consequence, the recovery increases.

Each point of the regression straight line reported in Fig. 9 can be obtained or fixing the feed flow rate and varying the feed pressure, or fixing the feed pressure and changing the feed flow rate. This implies the equivalence of the following relations:

$$\begin{aligned}&\text{Stage cut}^{A} = \text{stage cut}^{B}\\ &\Leftrightarrow \text{PermeateFlowRate}^{A}\\ &\quad = \text{PermeateFlowRate}^{B}\frac{\text{FeedFlowRate}^{A}}{\text{FeedFlowRate}^{B}}\end{aligned}$$

$$\begin{aligned}\text{H}_2\text{ recovered}^{A} &= \text{H}_2\text{ recovered}^{B}\\ &\Leftrightarrow \text{H}_2\text{ PermeateFlowRate}^{A}\\ &= \text{H}_2\text{ PermeateFlowRate}^{B}\\ &\quad\times\frac{\text{H}_2\text{ FeedFlowRate}^{A}}{\text{H}_2\text{ FeedFlowRate}^{B}}\end{aligned}$$

since H_2 concentrantion in the feed is the same

$$\begin{aligned}&\Leftrightarrow \text{H}_2\text{ PermeateFlowRate}^{A}\\ &\quad = \text{H}_2\text{ PermeateFlowRate}^{B}\frac{\text{FeedFlowRate}^{A}}{\text{FeedFlowRate}^{B}}\end{aligned}$$

In the stage cut range investigated, as a general concept, the higher the driving force (higher feed pressure) the higher the feed flow rate fraction (both H_2 and N_2) that permeates; however, at a high feed flow rate, the residence time of the stream with the membrane area is lower, therefore the advantage offered by the driving force is depleted and the H_2 recovery is lower. By the way, the H_2 flow rate in the permeate obtained at low feed flow rate and low feed pressure (Table 5-case A) is, in any case, lower than the one achieved at high pressure and high feed flow rate (Table 5-case B); however, their ratio (stage cut) is constant.

The hydrogen concentration in the permeate is strictly related to the stage cut (Fig. 10a). At a set feed pressure, a high stage cut implies the permeation of a larger fraction of the feed flow rate permeates through the membrane, but the retentate mixture is richer in N_2 and poorer in H_2 increasing the membrane length. In the second part of the membrane module N_2 permeates more with respect to

TABLE 5
Case studies comparing the hollow fiber module performances, at different operating conditions, for the same stage cut value

Case	Feed flow rate, dm^3(STP) h^{-1}	Feed pressure, bar	H_2 flow rate in the permeate, dm^3(STP) h^{-1}	H_2 recovery, %	Stage cut, %
	Example 1 – Average stage cut = ca. 7.6%				
A	1.7	4	0.13	22.3	7.3
B	3.9	6	0.35	24.8	8.0
	Example 2 – Average stage cut = ca. 14.7%				
A	0.6	4	0.078	35.6	14.0
B	1.7	6	0.260	42.7	15.4

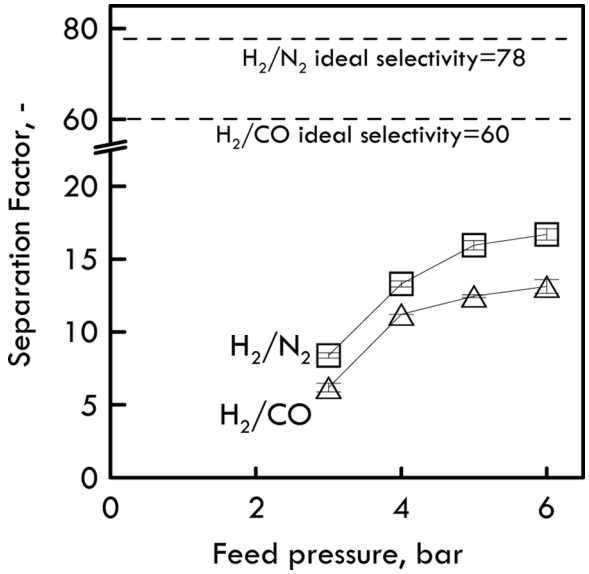

FIG. 11. Separation factor as a function of feed pressure for H_2:N_2 = 30:70 and H_2:CO = 30:70 mixtures. Feed flow rate = 2.8 dm^3(STP) h^{-1}.

the first section and thus dilutes the H_2 which permeated preferentially in the first part of the module. As a consequence, the higher the stage cut the lower the H_2 concentration. However, increasing the feed pressure, the H_2 partial pressure increases, therefore, for the same value of the stage cut, the concentration in the permeate increases as well. H_2 concentration versus the H_2 recovery (Fig. 10b) has the same trend shown with respect to the stage cut (Fig. 10a) owing to the linear relation between the recovery and the stage cut as demonstrated in Fig. 9.

For comparison with the results achieved with the mixture H_2:N_2 = 30:70, a mixture H_2:CO having the same composition was sent to the hollow fiber module. The experiments were carried out at the same operating conditions used for the first mixture, at a feed flow rate of 2.8 dm^3 (STP) h^{-1}. Figure 11 highlights the differences between the two mixtures in terms of separation factor. The curve correspondent to the mixture H_2:CO follows the same trend of that of the other mixture, showing an increase of separation factor with the feed pressure. This indicates that, in the range of operating condition considered, no differences in the behavior of the membrane versus the two different mixtures were observed. A higher separation factor was obtained when H_2 was mixed with N_2 rather than CO, in agreement with the trend followed

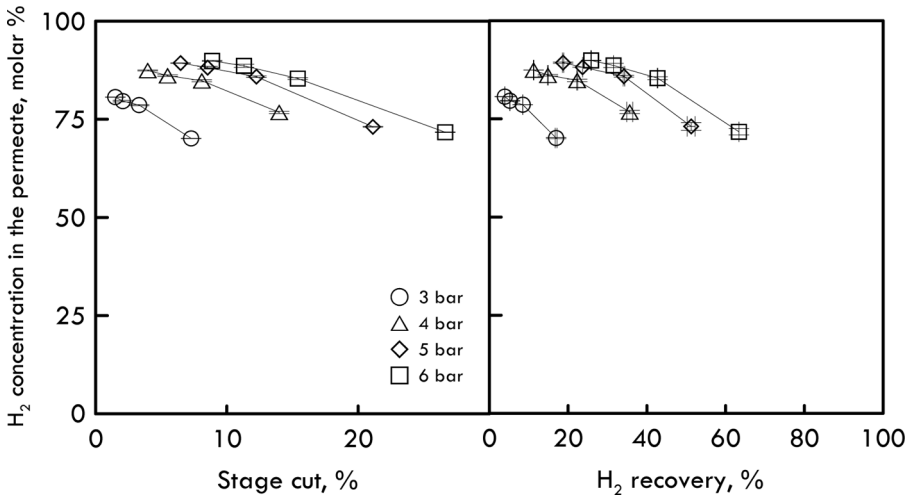

FIG. 10. H_2 concentration in the permeate as a function of stage cut and H_2 recovery, respectively, for different values of feed pressure. Mixture H_2:N_2 = 30:70.

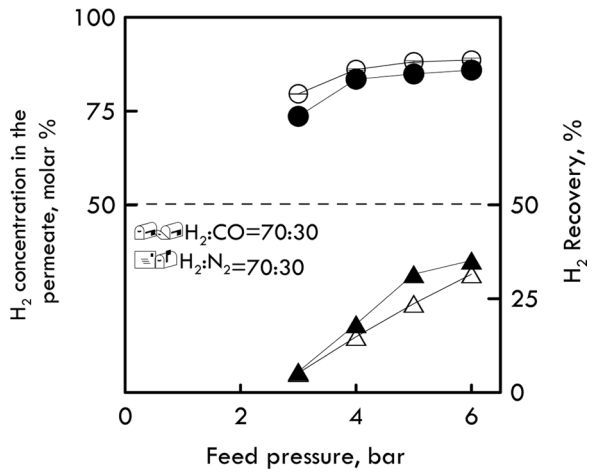

FIG. 12. H_2 concentration in the permeate and H_2 recovery as a function of Feed pressure for H_2:N_2 = 30:70 and H_2:CO = 30:70 mixtures. Feed flow rate = 2.8 dm^3(STP) h^{-1}.

by ideal selectivity values, since the one of H_2/N_2 was 78, a bit higher than that of H_2/CO (60).

In the whole feed pressure range, H_2 concentration in the permeate measured with the H_2:N_2 mixture was slightly higher than that obtained for the H_2 (Fig. 12):CO mixture, owing to the lower separation factor of this last mixture. However, for the same reason, an opposite trend was observed with the H_2 recovery, it being higher when the H_2 was mixed with CO.

Comparison of the Membrane Systems with the Traditional Separation Systems

Table 6 highlights the comparison among the performances of the membrane gas operation, considering the four different cases studies, with respect to the other two traditional separation units. The operating conditions considered for each case are that resumed in Table 2. First, comparing the case studies related to the membrane operation:

- Case 1 (experimental results), considers a higher H_2 recovery and a lower H_2 purity. As a consequence the installation area required is lower than Case 2 (experimental results), where a lower recovery but a higher H_2 purity are got. The mass intensity value obtained in both cases is significantly far from 1, which is the ideal condition. The mass intensity of case 1 is lower than the one of case two, owing to the lower hydrogen recovery. On the contrary, the productivity footprint is very close one to the other, basically due to the similar value of the installation area required.
- For case 3 and case 4, the same membrane properties and H_2 purity values of that measured and used in case 1 and case 2, respectively, were assumed, but considering the operation with a higher feed pressure (10 bar) and vacuum in the permeate side (0.2 bar). The correspondent values of H_2 recovery and stage cut were thus extrapolated considering the correlation reported in Fig. 9. In both cases, the direct consequence of the higher driving force was a significant reduction of the installation area with respect to case 1 and 2, respectively. As a consequence, a higher productivity footprint was obtained, as well as a lower mass intensity. Globally, the process becomes more intensified the higher the driving force. However, to confirm this idea, also the power required

TABLE 6
Comparison of membrane operation with traditional separation units. The data reported for PSA and cryogenic refers to (14)

	Membrane system (Case 1)	Membrane system (Case 2)	Membrane system (Case 3)	Membrane system (Case 4)	PSA	Cryogenic
Product flow rate, m^3 h^{-1}	3000	3000	3000	3000	2643	3375
H_2 recovery, molar%	64	26	85[a]	50[a]	73	90
H_2 purity, molar%	72	90	72[b]	90[b]	98	96
Installation area, m^2	55	56	21	18	60	120
Metrics						
Mass Intensity, kg kg_{H2}^{-1}	52.6	129.5	39.6	67.3	46.1	37.4
Productivity/footprint, kg $_{H2}$ h^{-1} m^{-2}	4.8	4.8	12.8	15	3.9	2.4

[a]Value linearly extrapolated considering the correlation reported in Fig. 8 for a stage cut of 35% and 20%, respectively.
[b]H_2 purity value assumed to be the same of cases 1 and 2, respectively.

for this operation with a higher driving force might be taken into account.

- The performances of the membrane system (all four cases) compared with the PSA and Cryogenic show interesting results. In particular, the installation area required by the membrane systems is always lower than the other two separation operations, and it is much more evident considering case 3 and 4. This reflects in a significantly higher productivity footprint ratio. However, the H_2 recovery and H_2 purity obtained with membrane operation are lower or comparable with the other two systems, therefore the mass intensity is higher. It must be pointed out that the membrane systems considered in these calculations operate at 50°C. However, at a higher temperature, the permeance of the membrane increases, therefore higher recovery can be expected. Moreover, the results presented by (13) for PSA and Cryogenic consider the treatment of a refinery off-gas, where the amount of hydrogen in the feed is higher (50–75%) (3) than that used in this work (30%).

CONCLUSIONS

A membrane module containing 165 hollow fibers made of P84® co-polyimide, was used in the separation of H_2/N_2 and H_2/CO mixtures. The measured permeance and separation factors showed relevant difference in comparison with that obtained feeding pure gases. The H_2 flux practically remained unchanged, whereas N_2 and CO fluxes showed significant increases. As a consequence, a separation factor ranging 9–18 and 6–12 was measured for the H_2/N_2 and H_2/CO mixtures, respectively, against an ideal selectivity of 78 and 60.

From the comparison with the literature results, the permeability shown by the P84-fiber prepared in this work well agrees with that measured by some other authors on a similar membrane, whereas H_2/N_2 ideal selectivity of the fiber was closer to or higher than the majority of those in other literature works.

Moreover, the differences between the transport properties measured on a single fiber and that measured with a hollow fiber module were taken into account. Comparing the permeance and selectivity measured considering the whole module with respect to that reported in the literature the P84 co-polyimide module shows significantly higher permeance values and H_2/N_2 ideal selectivity, very close to the one measured with the single fiber. This implies that the defects on the whole membrane surface are very few.

A linear dependence of the H_2 recovery on the stage cut was observed in the whole feed pressure range investigated. At low stage cut, only a small part of the hydrogen fed is recovered in the permeate, since the feed flow rate is oversized with respect to the membrane area available and, thus, to the extractive capacity of the membrane module; the higher the stage cut the higher the H_2 fraction recovered in the permeate.

No differences in the behavior of the membrane versus the two different mixtures were observed. The hydrogen-rich stream recovered in the permeate achieved interesting values of H_2 concentration up to 90% molar hydrogen purity. The performances of a membrane system showing the properties of the module realized in this work, were compared with that of the other separation operations actually used at industrial level such PSA and cryogenic, considering two metrics. In particular, the membrane systems showed a lower installation area with respect to the other two units, reaching interesting values of productivity-footprint ratio. This gain was much higher as the driving force was higher.

ACKNOWLEDGEMENTS

The EU-FP7 project "IMeTI - Implementation of Membrane Technology to Industry", "Grant Agreement Number PIAP-GA-2008–218068" is gratefully acknowledged for co-funding this work.

REFERENCES

1. Dautzenberg, F.; Mukherjee, M. (2001) Process intensification using multifunctional reactors. *Chem. Eng. Sci.*, 56: 251.
2. Stankiewicz, A.; Moulijn, J.A. (2002) Process intensification. *Ind. Eng. Chem. Res.*, 41 (8): 1920.
3. Miller, G.Q.; Stöcker, J. (1989) Selection of a hydrogen separation process *NPRA Annual Meeting*, San Francisco, California (USA).
4. Koros, W.J.; Pinnau, I. (1994) In: *Polymeric Gas Separation Membranes*, Paul, D.R.; Yampolskii, Y.P., eds.; CRC Press: Boca Raton, FL.
5. Park, H.B.; Kim, J.K.; Nam, S.Y.; Lee, Y.M. (2003) Imide-siloxane block copolymer/silica hybrid membranes: preparation, characterization and gas separation properties. *J. Mem. Sci.*, 220 (1–2): 59.
6. Grainger, D.; Hägg, M.B. (2007) Evaluation of cellulose-derived carbon molecular sieve membranes for hydrogen separation from light hydrocarbons. *J. Mem. Sci.*, 306 (1–2): 307.
7. Reverchon, E.; Cardea, S.; Schiavo Rappo, E. (2008) Membranes formation of a hydrosoluble biopolymer (PVA) using a supercritical CO_2-expanded liquid. *J. Supercr. Flu.*, 45 (3): 356.
8. Kapantaidakis, G.C.; Koops, G.H. (2002) High flux polyethersulfone–polyimide blend hollow fiber membranes for gas separation. *J. Mem. Sci.*, 204 (1–2): 153.
9. Barsema, J.N.; Kapantaidakis, G.C., v.d.; Vegt, N.F.A.; Koops, G.H.; Wessling, M. (2003) Preparation and characterization of highly selective dense and hollow fiber asymmetric membranes based on BTDA-TDI/MDI co-polyimide. *J. Mem. Sci.*, 216 (1–2): 195.
10. Ren, J.; Li, Z.; Wang, R. (2008) Effects of the thermodynamics and rheology of BTDA-TDI/MDI co-polyimide (P84) dope solutions on the performance and morphology of hollow fiber UF membranes. *J. Mem. Sci.*, 309 (1–2): 196.
11. Ren, J.; Li, Z.; Wong, F.-S. (2004) Membrane structure control of BTDA-TDI/MDI (P84) co-polyimide asymmetric membranes by wet-phase inversion process. *J. Mem. Sci.*, 241 (2): 305.
12. Peer, M.; Mahdeyarfar, M.; Mohammadi, T. (2009) Investigation of syngas ratio adjustment using a polyimide membrane. *Chem. Eng. Proc.*, 48 (3): 755.

13. Spillman, R.W. (1989) Economics of gas separation membranes. *Chem. Eng. Prog.*, 85: 41.
14. Yampolskii, Y.; Pinnau, I.; Freeman, B.D. (Eds.) (2006) *Materials Science of Membranes for Gas and Vapor separation*; Wiley: Chichester, 192–210.
15. Dalle Nogare, D. (2008) Modeling Catalytic Methane Partial Oxidation With Detailed Chemistry, PhD Thesis, Universita' Degli Studi Di Padova.
16. Curzons, A.D.; Constable, D.J.C.; Mortimera, D.N.; Cunningham, V.L. (2001) So you think your process is green, how do you know? Using principles of sustainablility to determine what is gree-a corporate perspective. *Green Chemistry*, 3: 1.
17. Martins, A.A.; Mata, T.M.; Costa, C.A.V.; Sikdar, S.K. (2007) Framework for sustainability metrics. *Ind. Eng. Chem. Res.*, 46 (10): 2962.
18. Bernardo, P.; Barbieri, G.; Drioli, E. (2010) Evaluation of membrane reactor with hydrogen-selective membrane in methane steam reforming. *Chem. Eng. Sci.*, 65 (3): 1159.
19. Jansen, J.C.; Buonomenna, M.G.; Figoli, A.; Drioli, E. (2006) Asymmetric membranes of modified poly(ether ether ketone) with an ultra-thin skin for gas and vapour separations. *J. Mem. Sci.*, 272 (1–2): 188.
20. Zhao, H.-Y.; Cao, Y.-M.; Ding, X.-L.; Zhou, M.-Q.; Yuan, Q. (2008) Effects of cross-linkers with different molecular weights in cross-linked Matrimid 5218 and test temperature on gas transport properties. *J. Mem. Sci.*, 323 (1): 176.
21. Favvas, E.P.; Kouvelos, E.P.; Romanos, G.E.; Pilatos, G.I.; Mitropoulos, A.Ch.; Kanellopoulos, N.K. (2008) Characterization of highly selective microporous carbon hollow fiber membranes prepared from a commercial co-polyimide precursor. *J. Porous Mater.*, 15 (6): 625.
22. Chatzidaki, E.K.; Favvas, E.P.; Papageorgiou, S.K.; Kanellopoulos, N.K.; Theophilou, N.V. (2007) New polyimide–polyaniline hollow fibers: Synthesis, characterization and behavior in gas separation. *Europ. Pol. J.*, 43 (12): 5010.